climate

MDPI

Article

IMERG-Based Meteorological Drought Analysis over Italy

Tommaso Caloiero [1,*], Giulio Nils Caroletti [2] and Roberto Coscarelli [2]

[1] Institute for Agricultural and Forest Systems in Mediterranean (CNR-ISAFOM), National Research Council, Via Cavour 4/6, 87036 Rende, Italy
[2] Research Institute for Geo-Hydrological Protection (CNR-IRPI), National Research Council, Via Cavour 4/6, 87036 Rende, Italy; iuliusscaevola@yahoo.it (G.N.C.); roberto.coscarelli@irpi.cnr.it (R.C.)
* Correspondence: tommaso.caloiero@isafom.cnr.it; Tel.: +39-0984-841464

Abstract: The Mediterranean region is an area particularly susceptible to water scarcity and drought. In this work, drought has been analyzed in Italy using multiple timescales of the standardized precipitation index (SPI) evaluated from the Integrated Multi-satellitE Retrievals for Global Precipitation Measurement product from 2000 to 2020. In particular, drought characteristics (severity, duration, and intensity) have been estimated by means of the run theory applied to the SPI values calculated in 3325 grid points falling within the Italian territory. Results clearly indicate that although a high number of drought events has been identified for the short timescale, these events present a lower duration and lesser severity than the long-timescale droughts. The main outcomes of this study, with the indication of the spatial distribution of the drought characteristics in Italy, allow identifying the areas that could also face water stress conditions in the future, thus requiring drought monitoring and adequate adaptation strategies.

Keywords: IMERG; drought; SPI; run theory; Italy

Citation: Caloiero, T.; Caroletti, G.N.; Coscarelli, R. IMERG-Based Meteorological Drought Analysis over Italy. *Climate* **2021**, *9*, 65. https://doi.org/10.3390/cli9040065

Academic Editor: Irina Repina

Received: 30 March 2021
Accepted: 14 April 2021
Published: 16 April 2021

1. Introduction

Although we are only twenty years into the 21st century, European and Mediterranean countries have already faced numerous drought events (e.g., in 2003, 2010, 2013, 2015, and 2018) [1], and a future increase in the number and the intensity of these events has been forecasted [2]. Drought events can severely impact water resources, agricultural production, and socio-economic activities, causing very costly damages [3]. As an example, widespread losses in agriculture and forestry have been registered in large parts of Europe after the 2018 drought event, which caused total damages of about €3.3 billion [4], and mainly hit Northern and Central Europe, including the UK and Scandinavia [5].

Drought events can occur in different ways and at different time intervals, thus different drought classifications have been proposed. One of the most common classifications considers four different droughts, i.e., meteorological (temporary lower-than-average precipitation), hydrological (scarcity in surface and subsurface water supplies), agricultural (water shortage compared with typical needs for crops irrigation), and socio-economic (referred to as global water consumption) droughts [6]. In order to monitor all the different types of droughts, researchers have developed several indices allowing them to assess the climate anomalies quantitatively in terms of intensity, duration, frequency, recurrence probability, and spatial extent [7]. Among the several indices, one of the most applied in the analysis of meteorological drought is the standardized precipitation index (SPI) which is a strong and effective drought index [8] enabling the analysis of different drought categories, and which can be evaluated for different timescales [9]. Moreover, the SPI is simpler to calculate than other indices, because its evaluation requires only rainfall data, and allows the comparison of meteorological drought events in different areas and for different time periods [10]. For these reasons, numerous studies have been performed using the SPI in several countries of the world, e.g., [11–15] and especially in the Mediterranean Basin, e.g., [16,17].

Among the different countries that have coastlines on the Mediterranean Sea, Italy can be considered especially interesting because of its location in the middle of the western Mediterranean and because it is characterized by a peculiar shape, extending over a wide latitude from north to south [18]. Mainly affected by a warm temperate Mediterranean climate with dry, warm summers (on average over 22 °C) and moderate wet winters, Italy is characterized by a Csa climate in the Koppen–Geiger classification [19]. Moreover, the Cfa climate characterizes the northern and northeastern areas of the country, which present humid conditions all year round. Several drought events affected Italy in the last decades, especially from 1980 onwards [20], and numerous studies on drought events have been carried out to analyze them [21–26]. The majority of these studies have been conducted at a regional scale, the main administrative division of the Italian State, and a comprehensive analysis at the national scale is missing due to the lack of a national database. In fact, since 1998, in Italy data collection is managed independently by individual regions. In recent years, the lack of spatially distributed data has been overcome thanks to the increased availability of meteorological satellites, which offered new opportunities for the regular monitoring of different climate variables. In particular, in recent decades, the precipitation data availability has been extensively improved by the development of remote sensing techniques at different spatial and temporal resolutions and satellite-based precipitation datasets have been largely applied for drought analysis and forecasting [27–31]. At present, several satellite precipitation products with large-scale coverage and high spatial and temporal resolutions are available, e.g., Climate Prediction Center morphing technique (CMORPH) precipitation; East Asian Multi-Satellite Integrated Precipitation (EMSIP); Precipitation Estimation from Remotely Sensed Information using Artificial Neural Networks (PERSIANN); Tropical Rainfall Measuring Mission's Multi-satellite Precipitation Analysis (TRMM-TMPA); Integrated Multi-satellitE Retrievals for Global Precipitation Measurement (IMERG). The suitability of these products for drought monitoring has been tested by several researchers. For example, in the Lancang River Basin, the authors of [32] evaluated the efficiency of TRMM-TMPA in drought monitoring during the 1998 to 2009 period, considering the 1- and 3-month SPI. In China, CMORPH-based SPI has been compared with the SPI evaluated using precipitation data from 2221 meteorological stations from 1998 to 2014, evidencing that the SPI evaluated from CMORPH precipitation could be applied to drought assessment and monitoring [33]. Finally, in South Korea the GPM IMERG-based SPI correlated well with the SPI evaluated from station precipitation observations [34].

The aim of this study is to perform a drought analysis using the SPI evaluated from GPM-based satellite precipitation estimates. With this aim, some of the main characteristics of the drought events that affected Italy from 2000 to 2020, such as quantity, duration, severity, and intensity have been analyzed. In this analysis, the use of satellite data allowed us to obtain a much more detailed distribution of the drought characteristics in Italy than those usually carried out by means of data from rain gauges, whose distribution is not homogenous on the whole territory.

2. Materials and Methods

2.1. IMERG Data

With the aim to provide an accurate and reliable estimation of the global precipitation using both active and passive microwave sensors, in 2014 NASA and JAXA launched the successor of the TRMM satellite i.e., the GPM mission [31]. GPM provides four levels of products based on different algorithms. The GPM level 3 products are the IMERG ones, which are characterized by high spatial ($0.1^\circ \times 0.1^\circ$) and temporal (30 min) resolution over the globe. IMERG provides three types of products: near-real-time Early Run (IMERG-E, with a latency of 4 h); reprocessed near-real-time Late Run (IMERG-L, with a latency of 14 h); gauged-adjusted Final Run (IMERG-F, with a latency of 3.5 months), which usually provides more precise precipitation datasets if compared to the previous two products [31]. Data used for this study were the monthly GPM IMERG Final Precipitation L3, Version 06B, provided on a $0.1^\circ \times 0.1^\circ$ (roughly 10×10 km) grid over the globe (https://disc.gsfc.nasa.

gov/datasets/GPM_3IMERGM_06/summary?keywords=%22IMERG%20final%22). The current period of record runs from June 2000 to the present, with the latest data available for November 2020, as of March 2021. In this paper, a 20-year time frame starting from December 2000 and running until November 2020 has been selected. Figure 1 shows the mean annual rainfall evaluated in the observation period for the 3325 grid points falling within the Italian territory.

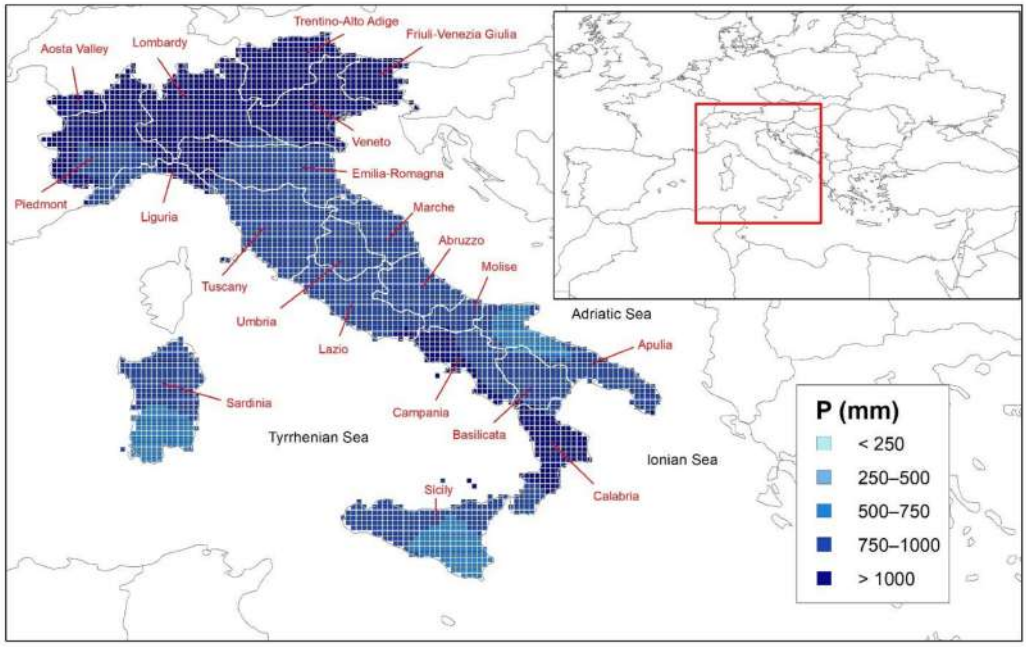

Figure 1. Localization of the study area and spatial distribution of the average annual precipitation from December 2000 to November 2020.

2.2. Standardized Precipitation Index

Following Angelidis et al. [35], in the SPI calculation, the gamma function has been considered as the more appropriate in fitting the frequency distribution of the cumulated precipitation at each timescale. Then, for each month of the year and for each time aggregation, the shape, and the scale parameters have been estimated using the approximation of Thom [36]. Moreover, in order to consider the zero values that occurred in the sample set and given that the gamma distribution is undefined for a null rainfall amount, a modified cumulative distribution function (CDF) has been used:

$$H(x) = q + (1 - q)G(x) \quad (1)$$

in which $G(x)$ is the CDF and q is the probability of zero precipitation, given by the ratio between the number of zero in the rainfall series (m) and the number of observations (n).

Finally, by using the approximate conversion provided by Abramowitz and Stegun [37], the CDF has been changed into the standard normal distribution:

$$z = SPI = -\left(t - \frac{c_0 + c_1 t + c_2 t^2}{1 + d_1 t + d_2 t^2 + d_3 t^3}\right),\ t = \sqrt{\ln\left(\frac{1}{(H(x))^2}\right)} \text{ for } 0 < \mathrm{H(x)} < 0.5 \quad (2)$$

$$z = SPI = +\left(t - \frac{c_0 + c_1 t + c_2 t^2}{1 + d_1 t + d_2 t^2 + d_3 t^3}\right),\ t = \sqrt{\ln\left(\frac{1}{(1 - H(x))^2}\right)} \text{ for } 0 < \mathrm{H(x)} < 0.5 \quad (3)$$

with c_0, c_1, c_2, d_1, d_2 and d_3 as mathematical constants.

Even though the first SPI classification, provided by McKee et al. [8], referred only to drought periods, nowadays SPI is also used in the classification of wet periods (Table 1).

Table 1. Climate classification according to the SPI values.

SPI Value	Class	Probability (%)
SPI $\geq$ 2.00	Extremely wet	2.3
1.5 $\leq$ SPI < 2.00	Severely wet	4.4
SPI < 1.50	Moderately wet	9.2
SPI < 1.00	Mildly wet	34.1
−1.00 $\leq$ SPI < 0.00	Mild drought	34.1
−1.50 $\leq$ SPI < −1.00	Moderate drought	9.2
−2.00 $\leq$ SPI < −1.50	Severe drought	4.4
SPI < −2.00	Extreme drought	2.3

2.3. Run Theory

The run theory proposed by Yevjevich [38] can be considered one of the most effective methods in the analysis of time series. The run theory refers to the occurrence of similar events, such as droughts, and allows characterizing each event by assessing some characteristics such as duration, severity, and intensity. An example of the run theory for a specified threshold level is shown in Figure 2 [39].

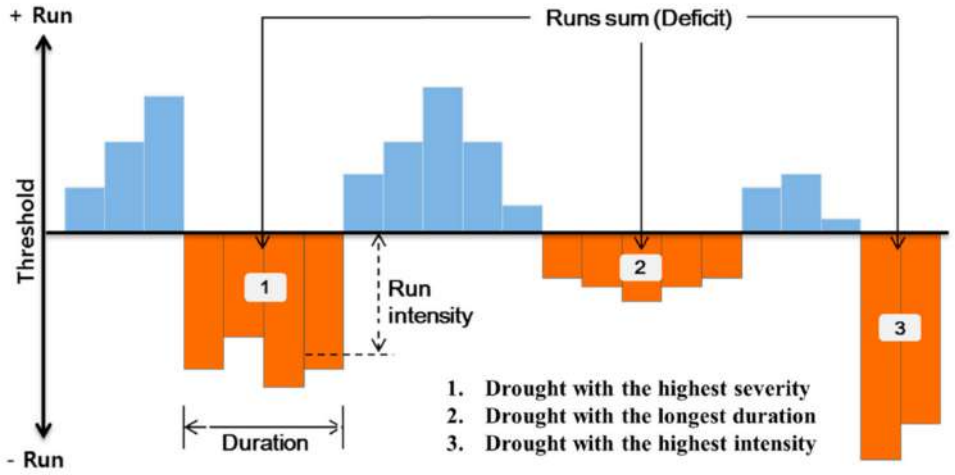

Figure 2. Example of the drought characteristics evaluated using run theory for a given threshold level [12].

The portions of the drought time series in which the values are all above or below the threshold are defined as "run" and are considered as positive or negative run, respectively [39]. Once the runs, and thus the drought events, have been identified it is possible to evaluate the different drought characteristics. The drought duration (*DD*) is the time period in which drought values are constantly below the threshold and can be expressed in weeks, months, years, or any other time period. The average drought duration (*ADD*) is the ratio between the sum of the *DD* of all the events and the number of events *N*. The cumulated drought values during each event represent the drought severity (*DS*). The average drought severity (*ADS*) is the ratio between the sum of the *DS* of all the events and *N*. The drought intensity (*DI*) is evaluated, for each event, as the ratio between *DS* and *DD*, thus the average drought intensity (*ADI*) is the ratio between the sum of the DI of all the events and *N*.

In this study, drought duration, severity, and intensity have been estimated using runs theory applied to the SPI series, and thus *DD* is expressed in months. This methodology has been largely applied in past studies performed for several areas of the world [40–42].

3. Results

In this study, dry periods were evaluated using the SPI at different timescales (3, 6, 12, and 24 months). In fact, while the 3- and 6-month SPI describe droughts that affect plant

life and farming, the 12- and 24-month SPI influence the way water supplies/reserves are managed [43,44].

By means of the boxplots in Figure 3, the main statistics of *N*, *ADD*, *ADS*, and *ADI* are shown for the different time scales (3, 6, 12, and 24 months). *N* obviously decreases with the increase of the time scale. In fact, in Italy, an average and a maximum of 19 and 27 events, respectively, have been detected in the observation period for the 3-month SPI, while, as regards the 24-months SPI, the average and the maximum number of events correspond to 6 and 15 events, respectively.

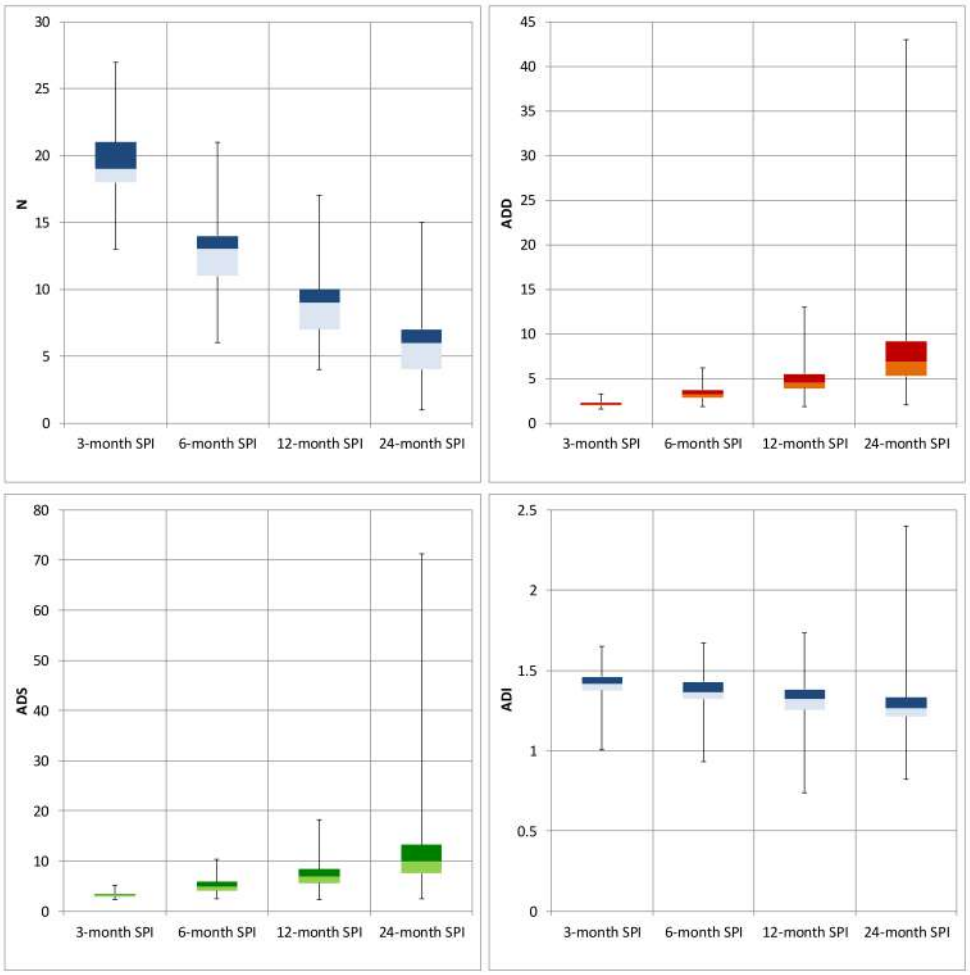

Figure 3. Characterization through boxplots of the number of drought events (*N*), average drought duration (*ADD*), average drought severity (*ADS*), and average drought intensity (*ADI*). The top and the bottom of the boxes are the third and the second quartiles, respectively; the band inside the box is the median and the ends of the whiskers represent the minimum and maximum of all of the data.

Figure 4 shows the spatial distribution of *N*. For the 3-month SPI the highest *N* values (also higher than 25) are localized in some parts of northern Italy (mainly in the Lombardy and the Piedmont regions), in a few areas of central Italy, and in a few regions of southern Italy (Campania, Sicily, and Sardinia). As regards the 6-month SPI, the highest *N* values are concentrated in northern Italy, reaching values higher than 20, and in a few areas of the Adriatic side of the Peninsula.

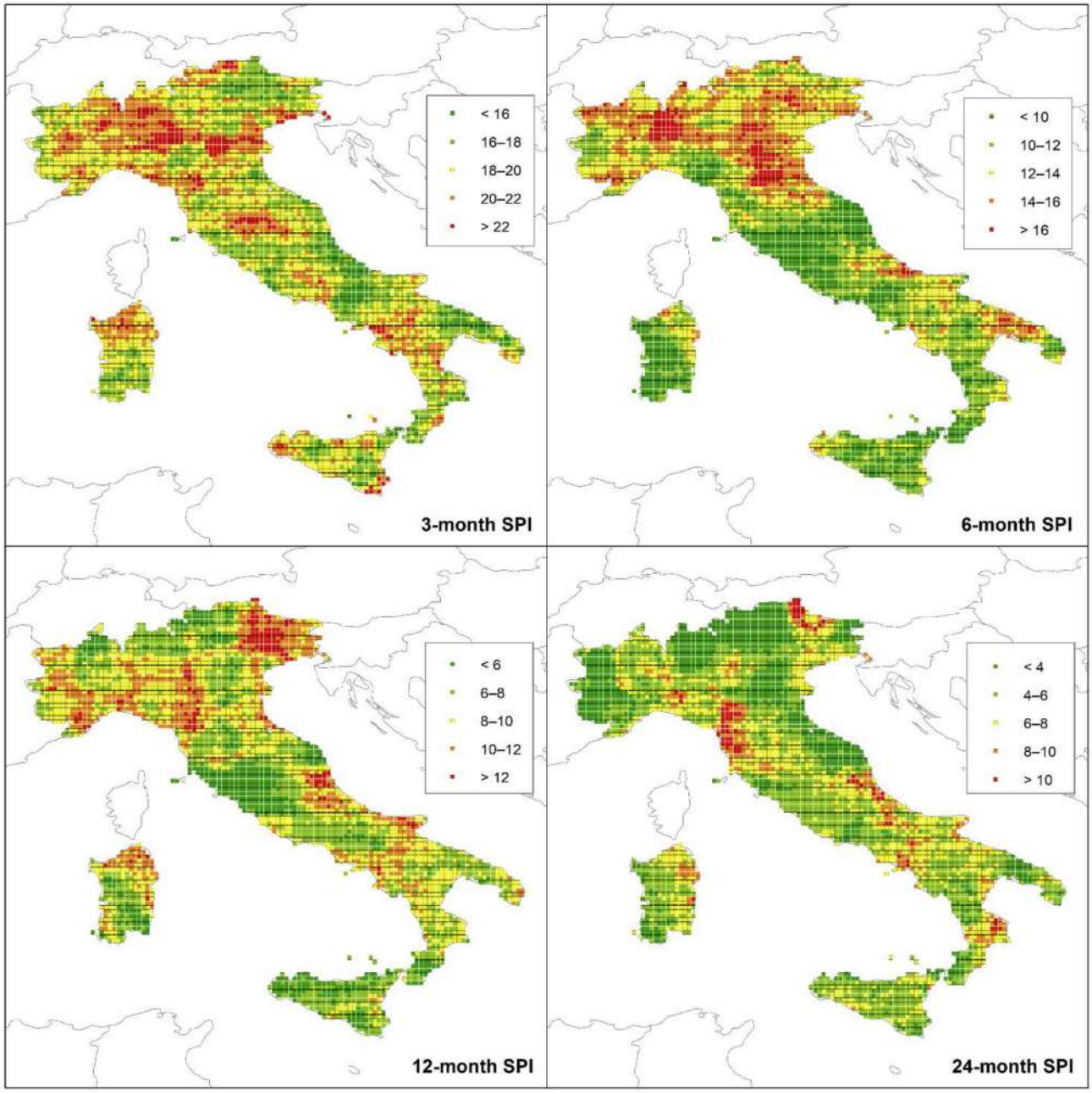

Figure 4. Spatial distribution of the number of drought events over Italy from 2000 to 2020.

The 12-month SPI distribution shows the highest number of events in the northeastern areas of the country, where a maximum of 17 events were identified during the observation period. High *N* values were also detected across northern Italy and in a few regions of central and southern Italy (Abruzzo and Apulia). As regards the longest timescale (24-month SPI) the highest *N* values have been identified in some areas of northern and central Italy (mainly in Trentino Alto Adige and Tuscany with a maximum of 14 and 15 events, respectively) and in a few cells in central Italy and on the Ionian side of the Calabria region (southern Italy).

The statistics of the *ADD* show an opposite behavior than *N* (Figure 3), with the lowest values corresponding to the 3-month SPI and the highest to the 24-month SPI. Although the average values do not show relevant differences among the various timescales (from about 2 months for the 3-month SPI to about 9 months for the 24-month SPI), different spreads are evident among the different scales. In fact, while for the 3-month SPI the *ADD* does not

present a large range of values (between 1.6 and 3.2 months), conversely, for the 24-month SPI the *ADD* maximum value reaches a value higher than 40 months. From the comparison between the spatial distributions of *ADD* (Figure 5) and *N* (Figure 4), it is evident that the more frequent events are those with the lowest durations.

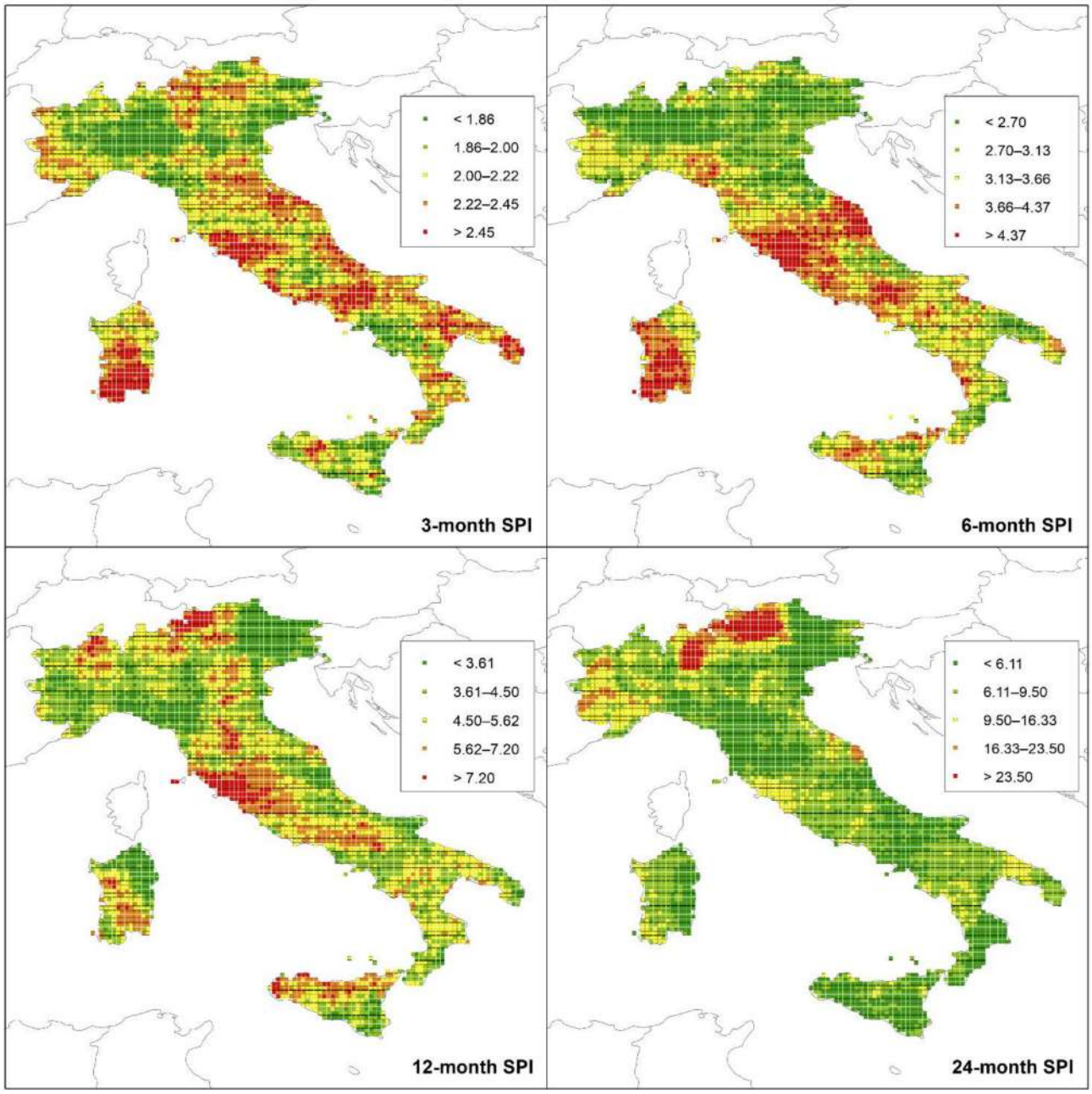

Figure 5. Spatial distribution of the average drought duration over Italy from 2000 to 2020.

As an example, for the 3-month SPI, the areas with the highest *ADD* (about 3 months) are concentrated in central Italy, in the southern side of Sardinia, and in a few cells of southern Italy (Figure 5) corresponding to almost all the areas presenting the lowest *N* values (Figure 4). This behavior is also evident for the drought events evaluated at the 6-, 12-, and 24-month time scale. As regards the 6-month SPI, the highest *ADD* values are localized in central Italy (>6 months) and in almost all of Sardinia. Few areas of central (between Lazio and Tuscany) and northern Italy (near the Alps) also present *ADD* values higher than 20 months, for the 12-month SPI. Finally, with respect to the 24-month SPI,

some areas of northern Italy (across Lombardy, Veneto, and Trentino Alto Adige) show very high *ADD* values, also greater than 40 months.

A behavior similar to *ADD* has been detected for the *ADS* for different temporal scales (Figure 3). The mean *ADS* value ranges from about 3 (3-month SPI) to almost 10 (24-month SPI). In addition, for the *ADS*, the spread increases with the temporal scale, with the minimum and the maximum values ranging from more than 2 to about 5 for the 3-month SPI and from about 2.5 to more than 71 for the 24-month SPI. The spatial distribution of the *ADS* is very similar to that of the *ADD* (Figure 6).

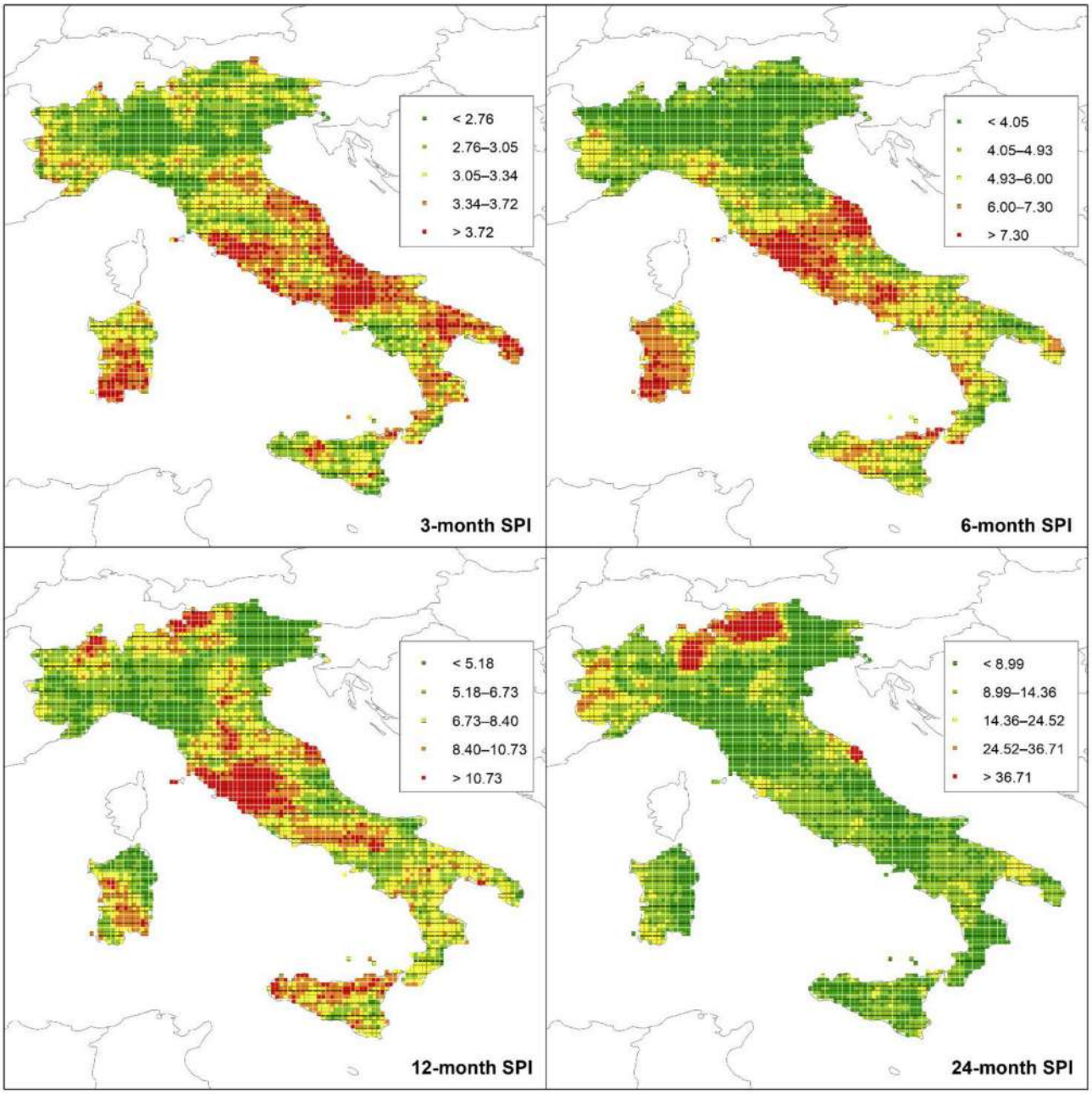

Figure 6. Spatial distribution of the average drought severity over Italy from 2000 to 2020.

This similarity means that the duration of the events greatly influences their severity. As regards the 3-month SPI the highest values of the *ADS* (>4) have been registered in some areas of central Italy and in Apulia. In northern Italy near the Alps, the *ADS* reachs values higher than 70 for the 24-month SPI (Figure 6).

Finally, Figure 3 shows that there are not many differences in the *ADI* values among the various temporal scales, with the average values ranging between 1.26 for the 24-month SPI and 1.4 for the 3-month SPI. As regards the 24-month SPI, the spread between the *ADI* values, ranging between 0.8 and about 2.4, was larger than the ones of the other time scales, ranging between 1 and 1.65, between 0.9 and 1.66, and between 0.73 and 1.73 for the 3-, 6- and 12-month SPI, respectively.

Figure 7 shows the spatial distribution of the *ADI* values in the Italian territory.

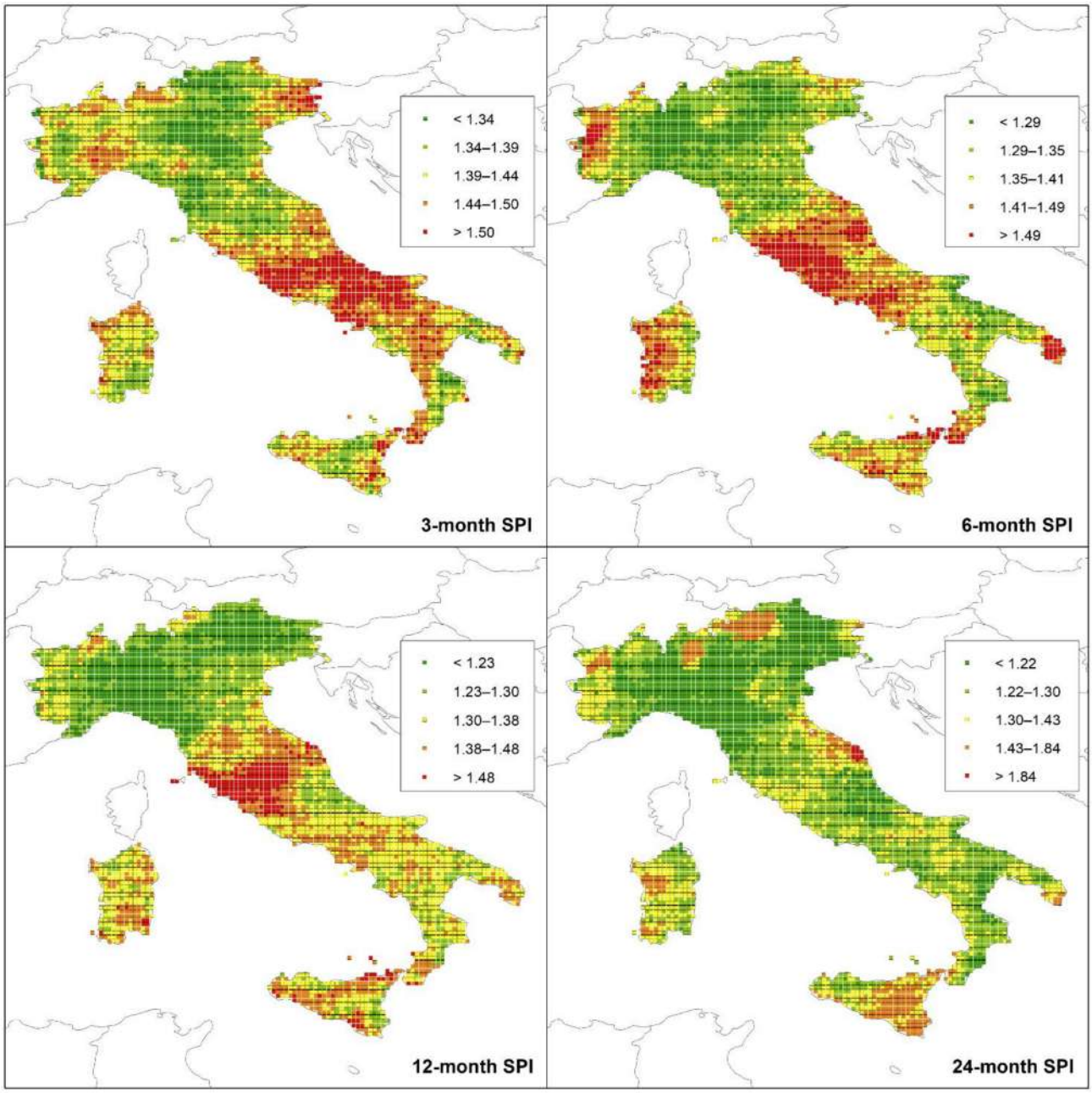

Figure 7. Spatial distribution of the average drought intensity over Italy from 2000 to 2020.

As a result, for almost all the time scales the highest *ADI* values are localized in large areas of central Italy, mainly in Tuscany and Lazio, reaching values higher than 1.6 for the 3- and 6-month SPI, and higher than 1.7 for the 12-month SPI. A different behavior characterizes the 24-month SPI, with the highest *ADI* values identified in a small area of the Adriatic side of central Italy (Marche region). Other cells with high *ADI* values have

been detected in the northeastern part of Italy and in a few areas of Apulia, Calabria, and Sicily for the 3-month SPI, in Sardinia, Calabria, Sicily, and Piedmont for the 6-month SPI, and in a few small areas of Sicily and Sardinia for the 12-month SPI.

4. Discussion

The Mediterranean region is an area particularly susceptible to water scarcity and drought. In fact, lack of precipitation is a normal part of the seasonal climatic cycle within the Mediterranean in summer. The summer drought depends on the strength and position of the Azores anticyclone and its eastward extension. In fact, when this anticyclone is well developed, drought is complete and may last for up to 4 months in southern Europe [44].

As climatic trends in droughts for the Mediterranean region point to the risk of water scarcity in southern Europe, the use of several drought indices and measures becomes increasingly important for the different needs of all those involved. While SPI trends can point to the change in precipitation distribution over the years, studying the number of droughts and of their characteristics is essential for politicians, local communities, and stakeholders in order to not only identify vulnerable areas, but also the drought features of the latter. With this aim, a spatially precise analysis can be achieved by exploiting increasingly available high-resolution, regular, satellite-based products like IMERG. This is especially important in areas like the Mediterranean, and especially Italy, where spatial variability in climate is high and local/regional climates greatly differ.

As IMERG is the de facto update of the TRMM database and project, its use is recommended in applications where TRMM proved a reliable data source. Even though high-resolution precipitation products like IMERG and TRMM are designed to provide the best precipitation estimates and not climate data records, studies that have analyzed the skill in TRMM in reproducing precipitation data showed good-to-excellent correlations (0.75-0.96) with ground-based data [45–47]. Comparing IMERG data for Italy with other studies of TRMM precipitation in the area, the strong correlation between TRMM and IMERG is clear [18].

Results are consistent with the most recent literature on Italian droughts. Hoerling et al. [48] showed an increase in drought episodes in the first decade of the 2000s. Spinoni et al. [20] showed that considering the 1952–2012 time period, the highest drought frequency, duration, and severity in the Mediterranean were reached in the 1990s and 2000s. Baronetti et al. [49] showed that since 2001, drought episodes in the Po valley (northern Italy) have become stronger in terms of frequency and length. These increases seem to correlate with changes in the intra-annual precipitation distribution, which in turn is dependent to some extent on teleconnection patterns, especially on the North Atlantic Oscillation [2,50].

5. Conclusions

The aim of this study was to analyze some of the main characteristics (quantity, duration, severity, and intensity) of the drought events that affected Italy between 2000 and 2020 using the SPI evaluated from GPM-based satellite precipitation estimates at short (3 and 6 months) and long (12 and 24 months) timescales. Generally, results evidenced that the number of drought events decreases with the increase of the time scales. On the contrary, an increase in the average drought duration and in the average drought severity has been detected with the increase of the time scales. As regards the average drought intensity, no particular changes have been identified among the various temporal scales. These results clearly indicate that considering the 3- and the 6-month SPI that refer to drought affecting vegetation and agricultural practices, several drought events could be expected, yet with short duration and little severity. Conversely, few but more severe drought events could hit the Italian territory when considering the 12- and 24-month SPI, which are a broad proxy for water resource management. Finally, from the spatial distribution of the drought characteristics, the national areas facing water stress were identified, thus evidencing that a strong strategy for adaptation is required, together with reliable monitoring and forecasting

systems for droughts. Further investigations could be conducted to improve the drought analysis by detecting more drought characteristics such as frequency, maximum duration, maximum severity, and maximum intensity.

Author Contributions: Conceptualization, T.C.; methodology, T.C. and G.N.C.; software, T.C. and G.N.C. formal analysis, T.C. and G.N.C.; validation: T.C. and R.C.; investigation, T.C. and G.N.C.; data curation, T.C. and G.N.C.; writing—original draft preparation, T.C. and R.C.; writing—review and editing, T.C., G.N.C. and R.C.; visualization, T.C.; supervision, T.C. All authors have read and agreed to the published version of the manuscript.

Funding: This research received no external funding.

Data Availability Statement: The data presented in this study are available on request from the corresponding authors.

Acknowledgments: The Project INDECIS is part of ERA4CS, an ERA-NET initiated by JPI Climate, and funded by FORMAS (SE), DLR (DE), BMWFW (AT), IFD (DK), MINECO (ES), ANR (FR) with co-funding by the European Union (Grant 690462).

Conflicts of Interest: The authors declare no conflict of interest.

References

1. Hanel, M.; Rakovec, O.; Markonis, Y.; Máca, P.; Samaniego, L.; Kyselý, J.; Kumar, R. Revisiting the recent European droughts from a long-term perspective. *Sci. Rep.* **2018**, *8*, 1–11. [CrossRef]
2. Caloiero, T.; Veltri, S.; Caloiero, P.; Frustaci, F. Drought Analysis in Europe and in the Mediterranean Basin Using the Standardized Precipitation Index. *Water* **2018**, *10*, 1043. [CrossRef]
3. Caloiero, T. SPI Trend Analysis of New Zealand Applying the ITA Technique. *Geosciences* **2018**, *8*, 101. [CrossRef]
4. MunichRe. The Natural Disasters of 2018 in Figures. Losses in 2018 Dominated by Wildfires and Tropical Storms. Available online: https://www.munichre.com/topics-online/en/climate-change-and-natural-disasters/natural-disasters/the-natural-disasters-of-2018-in-figures.html (accessed on 26 March 2021).
5. Peters, W.; Bastos, A.; Ciais, P.; Vermeulen, A. A historical, geographical and ecological perspective on the 2018 European summer drought. *Philos. Trans. R. Soc. Lond. B Biol. Sci.* **2020**, *375*, 20190505. [CrossRef]
6. Zargar, A.; Sadiq, R.; Naser, B.; Khan, F.I. A review of drought indices. *Environ. Rev.* **2011**, *19*, 333–349. [CrossRef]
7. Tsakiris, G.; Pangalou, D.; Vangelis, H. Regional drought assessment based on the Reconnaissance Drought Index (RDI). *Water Resour. Manag.* **2007**, *21*, 821–833. [CrossRef]
8. McKee, T.B.; Doesken, N.J.; Kleist, J. The relationship of drought frequency and duration to time scales. In Proceedings of the 8th Conference on Applied Climatology, Anaheim, CA, USA, 17–22 January 1993; pp. 179–184.
9. Capra, A.; Scicolone, B. Spatiotemporal variability of drought on a short–medium time scale in the Calabria Region (Southern Italy). *Theor. Appl. Climatol.* **2012**, *3*, 471–488. [CrossRef]
10. Caloiero, T.; Coscarelli, R.; Ferrari, E.; Sirangelo, B. An Analysis of the Occurrence Probabilities of Wet and Dry Periods through a Stochastic Monthly Rainfall Model. *Water* **2016**, *8*, 39. [CrossRef]
11. Caloiero, T. Drought analysis in New Zealand using the standardized precipitation index. *Environ. Earth Sci.* **2017**, *76*, 569. [CrossRef]
12. Lee, S.-H.; Yoo, S.-H.; Choi, J.-Y.; Bae, S. Assessment of the Impact of Climate Change on Drought Characteristics in the Hwanghae Plain, North Korea Using Time Series SPI and SPEI: 1981–2100. *Water* **2017**, *9*, 579. [CrossRef]
13. Pei, Z.; Fang, S.; Wang, L.; Yang, W. Comparative Analysis of Drought Indicated by the SPI and SPEI at Various Timescales in Inner Mongolia, China. *Water* **2020**, *12*, 1925. [CrossRef]
14. Bong, C.H.J.; Richard, J. Drought and climate change assessment using Standardized Precipitation Index (SPI) for Sarawak River Basin. *J. Water Clim. Chang.* **2020**, *11*, 956–965. [CrossRef]
15. Khosravi, H.; Haydari, E.; Shekoohizadegan, S.; Zareie, S. Assessment the Effect of Drought on Vegetation in Desert Area using Landsat Data. *Egypt. J. Remote Sens. Space Sci.* **2017**, *20*, S3–S12. [CrossRef]
16. Magno, R.; Pasqui, M.; Di Giuseppe, E. Analysis of changes in drought occurrence over the Mediterranean Basin using multiple time scales SPI index. In Proceedings of the 16th EMS Annual Meeting & 11th European Conference on Applied Climatology (ECAC), Trieste, Italy, 12–16 September 2016.
17. Cavus, Y.; Aksoy, H. Spatial Drought Characterization for Seyhan River Basin in the Mediterranean Region of Turkey. *Water* **2019**, *11*, 1331. [CrossRef]
18. Caloiero, T.; Caroletti, G.N.; Coscarelli, R. TRMM-based rainfall temporal analysis over Italy. *SN Appl. Sci.* **2020**, *2*, 1270. [CrossRef]
19. Köppen, W. *Das Geographische System der Klimate. Handbuch der Klimatologie*; Köppen, W., Geiger, R., Eds.; Verlag von Gebrüder Borntraeger: Berlin, Germany, 1936; Volume 1, pp. 1–44.

20. Spinoni, J.; Naumann, G.; Vogt, J.V.; Barbosa, P. The biggest drought events in Europe from 1950 to 2012. *J. Hydrol. Reg. Stud.* **2015**, *3*, 509–524. [CrossRef]
21. Bonaccorso, B.; Bordi, I.; Cancelliere, A.; Rossi, G.; Sutera, A. Spatial variability of drought: An analysis of SPI in Sicily. *Water Resour. Manag.* **2003**, *17*, 273–296. [CrossRef]
22. Mendicino, G.; Senatore, A.; Versace, P. A Groundwater Resource Index (GRI) for drought monitoring and forecasting in a Mediterranean climate. *J. Hydrol.* **2008**, *357*, 282–302. [CrossRef]
23. Vergni, L.; Todisco, F. Spatio-temporal variability of precipitation temperature and agricultural drought indices in Central Italy. *Agric. For. Meteorol.* **2011**, *151*, 301–313. [CrossRef]
24. Capra, A.; Consoli, S.; Scicolone, B. Long-term climatic variability in Calabria and effects on drought and agrometeorological parameters. *Water Resour. Manag.* **2013**, *27*, 601–617. [CrossRef]
25. Caloiero, T.; Coscarelli, R.; Ferrari, E.; Sirangelo, B. Occurrence Probabilities of Wet and Dry Periods in Southern Italy through the SPI Evaluated on Synthetic Monthly Precipitation Series. *Water* **2018**, *10*, 336. [CrossRef]
26. Caloiero, T.; Veltri, S. Drought Assessment in the Sardinia Region (Italy) During 1922–2011 Using the Standardized Precipitation Index. *Pure Appl. Geophys.* **2019**, *176*, 925–935. [CrossRef]
27. Toté, C.; Patricio, D.; Boogaard, H.; van der Wijngaart, R.; Tarnavsky, E.; Funk, C. Evaluation of Satellite Rainfall Estimates for Drought and Flood Monitoring in Mozambique. *Remote Sens.* **2015**, *7*, 1758–1776. [CrossRef]
28. Fan, F.M.; Collischonn, W.; Quiroz, K.; Sorribas, M.; Buarque, D.; Siqueira, V. Flood forecasting on the Tocantins River using ensemble rainfall forecasts and real-time satellite rainfall estimates. *J. Flood Risk Manag.* **2016**, *9*, 278–288. [CrossRef]
29. Zambrano, F.; Wardlow, B.; Tadesse, T.; Lillo-Saavedra, M.; Lagos, O. Evaluating satellite-derived long-term historical precipitation datasets for drought monitoring in Chile. *Atmos. Res.* **2017**, *186*, 26–42. [CrossRef]
30. Gao, F.; Zhang, Y.; Ren, X.; Yao, Y.; Hao, Z.; Cai, W. Evaluation of CHIRPS and its application for drought monitoring over the Haihe River Basin, China. *Nat. Hazard* **2018**, *92*, 155–172. [CrossRef]
31. Zhu, Q.; Luo, Y.; Zhou, D.; Xu, Y.-P.; Wang, G.; Gao, H. Drought Monitoring Utility using Satellite-Based Precipitation Products over the Xiang River Basin in China. *Remote Sens.* **2019**, *11*, 1483. [CrossRef]
32. Zeng, H.; Li, L.; Li, J. The evaluation of TRMM Multisatellite Precipitation Analysis (TMPA) in drought monitoring in the Lancang River Basin. *J. Geogr. Sci.* **2012**, *22*, 273–282. [CrossRef]
33. Lu, J.; Jia, L.; Menenti, M.; Yan, Y.; Zheng, C.; Zhou, J. Performance of the Standardized Precipitation Index Based on the TMPA and CMORPH Precipitation Products for Drought Monitoring in China. *IEEE J. Sel. Top. Appl. Earth Obs. Remote Sens.* **2018**, *11*, 1387–1396. [CrossRef]
34. Jang, S.; Center, A.C.; Rhee, J.; Center, A.C.; Yoon, S.; Center, A.C.; Lee, T.; Park, K.; Center, A.C. Evaluation of GPM IMERG Applicability Using SPI based Satellite Precipitation. *J. Korean Soc. Agric. Eng.* **2018**, *59*, 29–39.
35. Angelidis, P.; Maris, F.; Kotsovinos, N.; Hrissanthou, V. Computation of drought index SPI with Alternative Distribution Functions. *Water Resour. Manag.* **2012**, *26*, 2453–2473. [CrossRef]
36. Thom, H.C.S. A note on the gamma distribution. *Mon. Weather Rev.* **1958**, *86*, 117–122. [CrossRef]
37. Abramowitz, M.; Stegun, I.A. *Handbook of Mathematical Functions with Formulas, Graphs, and Mathematical Tables*; Dover Publications, Inc.: New York, NY, USA, 1970.
38. Yevjevich, V. An Objective Approach to Definitions and Investigation of Continental Hydrologic Droughts. In *Hydrology Paper 23*; Colorado State University: Fort Collins, CO, USA, 1967.
39. Mishra, A.K.; Singh, V.P. A review of drought concepts. *J. Hydrol.* **2010**, *391*, 202–216. [CrossRef]
40. Wu, R.; Zhang, J.; Bao, Y.; Guo, E. Run Theory and Copula-Based Drought Risk Analysis for Songnen Grassland in Northeastern China. *Sustainability* **2019**, *11*, 6032. [CrossRef]
41. Liu, X.; Wang, S.; Zhou, Y.; Wang, F.; Li, W.; Liu, W. Regionalization and Spatiotemporal Variation of Drought in China Based on Standardized Precipitation Evapotranspiration Index (1961–2013). *Adv. Meteorol.* **2015**, *2015*, 950262. [CrossRef]
42. Da Rocha, R.L., Jr.; dos Santos Silva, F.D.; Costa, R.L.; Gomes, H.B.; Pinto, D.D.C.; Herdies, D.L. Bivariate Assessment of Drought Return Periods and Frequency in Brazilian Northeast Using Joint Distribution by Copula Method. *Geosciences* **2020**, *10*, 135. [CrossRef]
43. Buttafuoco, G.; Caloiero, T.; Ricca, N.; Guagliardi, I. Assessment of drought and its uncertainty in a southern Italy area (Calabria region). *Measurement* **2018**, *113*, 205–210. [CrossRef]
44. Oliver, J.E. *Encyclopedia of World Climatology*; Springer: Amsterdam, The Netherlands, 2005.
45. Kalimeris, A.; Kolios, S. TRMM-based rainfall variability over the Central Mediterranean and its relationships with atmosphric and oceanic climate models. *Atmos. Res.* **2019**, *230*, 104649. [CrossRef]
46. Nastos, P.T.; Kaposmenakis, J.; Philandras, K.M. Evaluation of the TRMM 3B43 gridded rainfall estimates over Greece. *Atmos. Res.* **2016**, *169*, 497–514. [CrossRef]
47. Kolios, S.; Kalimeris, A. Evaluation of the TRMM rainfall product accuracy over the central Mediterranean during a 20-year period. *Theor. Appl. Climatol.* **2020**, *139*, 785–799. [CrossRef]
48. Hoerling, M.; Eischeid, J.; Perlwitz, J.; Quan, X.; Zhang, T.; Pegion, P. On the increased frequency of Mediterranean drought. *J. Clim.* **2012**, *25*, 2146–2161. [CrossRef]

49. Baronetti, A.; González-Hidalgo, J.C.; Vicente-Serrano, S.M.; Acquaotta, F.; Fratianni, S. A weekly spatio-temporal distribution of drought events over the Po Plain (North Italy) in the last five decades. *Int. J. Climatol.* **2020**, *40*, 4463–4476. [CrossRef]
50. Vicente-Serrano, S.M.; López-Moreno, J.I.; Lorenzo-Lacruz, J.; El Kenawy, A.; Azorin-Molina, C.; Morán-Tejeda, E.; Pasho, E.; Zabalza, J.; Begueria, S.; Angulo-Martinez, M. The NAO impact on droughts in the Mediterranean region. In *Hydrological, Socioeconomic and Ecological Impacts of the North Atlantic Oscillation in the Mediterranean Region Advances in Global Change Research*; Springer: Dordrecht, The Netherlands, 2011.